Available online at www.eccomasproceedia.org
Eccomas Proceedia COMPDYN (2023) 285-295

ECCOMAS Proceedia

COMPDYN 2023
9th ECCOMAS Thematic Conference on
Computational Methods in Structural Dynamics and Earthquake Engineering
M. Papadrakakis, M. Fragiadakis (eds.)
Athens, Greece, 12-14 June 2023

SEISMIC PROTECTION OF CULTURAL HERITAGE BUILDING CONTENTS BY KINEMATIC ISOLATION DEVICES

Gabriele Guerrini[1,2], Francesco Graziotti[1,2], Maria Rota[2], and Andrea Penna[1,2]

[1] Department of Civil Engineering and Architecture
University of Pavia
Via Ferrata, 3 - 27100, Pavia (PV) - Italy
gabriele.guerrini@unipv.it, francesco.graziotti@unipv.it, andrea.penna@unipv.it

[2] EUCENTRE Foundation
Via Ferrata, 3 - 27100, Pavia (PV) - Italy
maria.rota@eucentre.it

Abstract

The University of Pavia and the EUCENTRE Foundation in Italy conducted an experimental study to evaluate the effectiveness of a new seismic isolation device in protecting cultural heritage building contents. The device, called "Kinematic Steel Joint (KSJ)", is made entirely of steel components and uses a multiple articulated quadrilateral mechanism. The KSJ isolator can be manufactured in different sizes, payloads, and displacement ranges, making it suitable for global building-level seismic isolation or local non-structural component protection. While current isolation devices effectively reduce seismic accelerations, they can add to construction costs and may require specific maintenance. The KSJ solution, on the other hand, offers a reduction in manufacturing and maintenance burdens. This paper presents the results of a shake-table test using four prototypes of the KSJ device. The test involved a rigid mass supported by the isolators, two marble blocks representing nonstructural components, a museum showcase with a small-scale replica of Michelangelo's David, and two clay vases. Accelerometers and potentiometers were used to monitor the kinematic response of the isolators and their effect on the dynamic response of the rigid mass and different nonstructural elements. The experiment was conducted both with and without seismic isolation, to compare the response of the non-structural components and understand the effect of the KSJ devices on the overall test assembly and sub-components. The influence of the vertical earthquake component in fixed-base conditions was also investigated.

Keywords: Cultural heritage, Kinematic steel joint, Non-structural components, Seismic isolation, Shake-table test.

Peer-review under responsibility of the organizing committee of COMPDYN 2023.
doi: 10.7712/120123.10405.20726

1 INTRODUCTION

Earthquake-induced cyclic accelerations on buildings can result in damage to both structural and nonstructural components, which can ultimately lead to partial or total collapse. While the current seismic design philosophy focuses on the concept of structural ductility, which allows structures to deform beyond their elastic limit to prevent collapse [1], protecting buildings from earthquakes also requires limiting the economic and social cost of post-event disruption, repair, and reconstruction. Seismic isolation technologies have emerged as an alternative approach to traditional ductile design, with the goal of limiting the potential damage to the built environment, particularly true when valuable contents are to be preserved, such as cultural heritage, technological, or hospital assets [2]–[6].

Seismic isolation is typically achieved through the creation of an isolation layer, which acts as a filter for the seismic input to reduce acceleration, displacement, and deformation demand on a building's elements and contents. Isolation can be integrated into new buildings or added to existing structures as a retrofit solution. The most common form of seismic isolation is base isolation, which is typically provided at the basement level or crawl space of buildings, although it can also be applied to higher locations depending on the building configuration or which portions require special protection [7]. Isolation can be limited to specific building areas, such as floating floors supported on seismic isolators installed only in selected rooms, to protect valuable contents [8]–[9]. Individual nonstructural elements and contents can also be isolated from ground or floor accelerations in some cases [10]–[16].

A typical base isolation system requires low lateral stiffness, the ability to dissipate energy, and the ability to recenter to its at-rest position at the end of the seismic excitation. Elastomeric and friction pendulum bearings are the most used isolators for building structures, but other types of isolators such as rollers or suspension systems can also provide satisfactory performance in combination with independent energy dissipators and recentering devices [17]. A drawback of conventional seismic isolation is sometimes represented by the higher construction cost and the need for specific maintenance or replacement over time, which in turn requires access to isolators and energy dissipators to control their performance [18]–[22].

To address these issues, Kyneprox S.r.l. has developed a new type of isolator, the Kinematic Steel Joint (KSJ), which consists of a double articulated quadrilateral with crossing rods entirely made of steel. The device provides recentering pendulum-type motion to the superstructure and energy dissipation due to friction within pin connections between its members [23]. The KSJ can be produced with different sizes, payloads, and displacement capacities, making it suitable for a variety of applications ranging from non-structural content to entire building isolation [24]–[25]. Stainless or galvanized steel can be used for practical implementations, to reduce corrosion sensitivity.

This paper discusses the results of a shake-table test conducted at the EUCENTRE Foundation laboratories on an assembly with four KSJ devices, a rigid mass simulating the building superstructure, and several components representing cultural heritage assets.

2 KSJ PROTOTYPE

This study validated the KSJ prototype shown in Fig. 1, which was made of S235 steel rods and plates. Durability was not a concern for the experimental campaign, but for commercial devices, stainless or galvanized steel would be used to tackle corrosion issues. All rods and plates were obtained from 10-mm-thick steel sheets, with notches and chamfers to accommodate the maximum rod rotations corresponding to the displacement capacity of the device. The connections between members consisted of bolts and thrust bearings, which acted as pins with some frictional resistance.

Figure 1: Prototype of the Kinematic Steel Joint (KSJ) isolator.

The device had top and bottom square plates with 400-mm side, which allowed connecting the device to the shake-table and to the rigid mass. The prototype had three modules mounted side by side in parallel, each consisting of four diagonal rods crossing in pairs and a horizontal rod. The top and bottom ends of the diagonal rods were pinned to vertical plates, fillet-welded to the horizontal plates and shaped compatibly with the pendulum-type motion of the device and the maximum rod rotations.

To prevent transverse and torsional deviations, the prototype had a restraining system consisting of rigid steel plates and cylindrical bearings. To allow full two-dimensional motion in a horizontal plane, two devices with orthogonal orientation could be combined on top of each other for practical applications. Aligning multiple KSJ isolators fixed to the shake-table and to the rigid superstructure mass resulted in a single-degree-of-freedom system with pendulum-type motion, as the rotation of the top horizontal plate was prevented.

An analytical study was performed on the device to establish its kinematic, static, and dynamic properties [23]. The behavior was characterized by a variable-curvature trajectory with restoring force proportional to the local slope and lateral stiffness proportional to the local curvature. The average radius of curvature R, for a given lateral displacement, is defined as the radius of the circle passing through the at-rest position and the symmetrical points at the positive and negative displacement of interest along the trajectory. The average period T_b of the isolated system is obtained from the average radius R as for a simple pendulum, independently of the mass (assumed rigid).

The lateral response of the KSJ isolator was affected by geometric variations due to gravity loading: the maximum horizontal displacement slightly reduced from ±130 mm to ±121 mm, while the trajectory became steeper, and the lateral stiffness increased. Consequently, the average isolation period at 80-mm lateral displacement reduced from 2.1 s to 1.8 s. Fig. 2 shows the analytical response of the KSJ prototype, including trajectories of an individual device and lateral force-displacement envelopes for a superstructure weight of 205 kN.

3 INCREMENTAL DYNAMIC SHAKE-TABLE TESTS

3.1 Specimen and setup

The KSJ isolation effectiveness was assessed through a dynamic shake-table test at the 6DLab of the EUCENTRE Foundation in Pavia, Italy. The test involved four in-parallel devices that supported a 205-kN mass, mainly coming from a 158-kN reinforced concrete (RC) block resting on two 10.1-kN longitudinal HE 400 B steel beams, supported by two KSJ each (Fig. 3a). Additional mass was provided by four 0.4-kN steel adaptor plates.

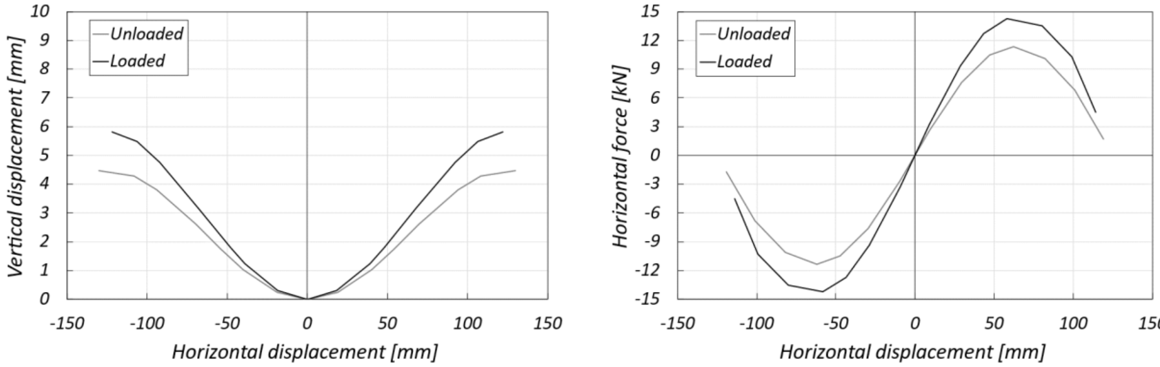

(a) (b)

Figure 2: Predicted KSJ response with or without geometric variations due to loading: (a) trajectories of a device; (b) lateral force-displacement backbone curves under a superstructure weight of 205 kN.

(a) (b)

Figure 3: Shake-table test specimen and setup: (a) isolators, steel beam, main RC block, steel guide, and safety A-brace; (b) nonstructural components.

A museum showcase provided by Goppion S.p.A. with a weight of 2.5 kN was placed on top of the main mass along with a small-scale 3D-printed replica of Michelangelo's David statue and two clay vases with negligible mass (Fig. 3b). The nonstructural elements also included two marble blocks used to simulate rocking heritage components. One block, referred to as the "free-rocking block", weighed 4 kN and had a semi-diagonal of 0.791 m and a slenderness angle with tangent equal to 0.203. The second block, identified as the "one-side-rocking block", weighed 4 kN and had a semi-diagonal of 0.779 m and a slenderness angle with tangent equal to 0.103.

Steel guides were placed below the longitudinal HE 400 B beams to prevent transverse and torsional motion in case of out-of-plane restraint failure (Fig. 3a). Two safety steel A-braces were provided to stop the mass if the KSJ devices or connections failed after reaching the maximum longitudinal displacement allowance.

3.2 Instrumentation

Accelerometers, potentiometers, and wire potentiometers were installed on all components of the setup. The shake-table platen had a triaxial accelerometer at its center, while the reinforced concrete block had two triaxial accelerometers on its East and West sides. Triaxial accelerometers were also attached to each moving marble block, while uniaxial sensors were provided to the conic base and the fixed block.

Characteristic	EMN	CIN
Date	29/05/2012	30/10/2016
Time	06:40:18	07:00:02
Moment magnitude	6.0	6.5
Province	Modena	Perugia
Municipality	Finale Emilia	Preci
Latitude [°]	44.8486	42.8793
Longitude [°]	11.2479	13.0334
Rupture distance [km]	6.68	8.95
Horizontal component	North	North
Horizontal PGA [g]	0.254	0.310
Vertical PGA [g]	0.315	0.181

Table 1: Input motion characteristics.

Three potentiometers per KSJ device were used to record the isolator motion and to verify the efficiency of the out-of-plane restraint. Two wire potentiometers recorded the displacements of the rocking marble blocks. Two potentiometers were also used to check for sliding between the RC block and the steel beams.

3.3 Testing protocol

Three series of incremental dynamic tests were conducted: one in base isolated conditions, the other two with fixed base by blocking the relative displacement between RC block and table platen. The tests used two natural-seismicity ground-motion records from the Italian database ITACA (ITalian ACcelerometric Archive) [26]. The first signal, EMN, was from the 2012 Emilia earthquake sequence, and the second one, CIN, was from the 2016 Central Italy seismic events (Table 1).

Only one horizontal component of each record was applied to the base-isolated test series, with amplitude scaling ranging from 25% to 250%. The first fixed-base test sequence used the same EMN record scaled up to 200% and the CIN input scaled up to 125% to avoid showcase damage. The second fixed-base test series included the vertical ground-motion component, with the same scaling factors as the horizontal component, with maximum scale factors of 175% for EMN and 150% for CIN.

In the upcoming sections, each stage of the incremental dynamic test will be denoted by the three letters of the signal label, such as EMN or CIN, followed by the percentage of acceleration amplitude scaling. The suffixes ISO, FIX, or FIX-Z will be used to indicate the base-isolated test series, the fixed-base series with only horizontal input, and the fixed-base series with both horizontal and vertical components, respectively.

4 EXPERIMENTAL RESULTS

4.1 KSJ isolator performance

Fig. 4a displays the trajectories of the four KSJ isolators during the CIN250%-ISO test, showing a pendulum-type motion with variable curvature, in good agreement with the analytical prediction. Isolators 1 and 2 experienced maximum horizontal displacements of about 80 mm, resulting in an upward displacement of nearly 4 mm. Isolators 3 and 4 had a slightly shifted trajectory to the left, likely due to initial misalignment during setup assembly. The analytical model did not predict the isolator downward settlement, which stabilized with residual vertical displacements ranging between 0.2 mm and 0.6 mm.

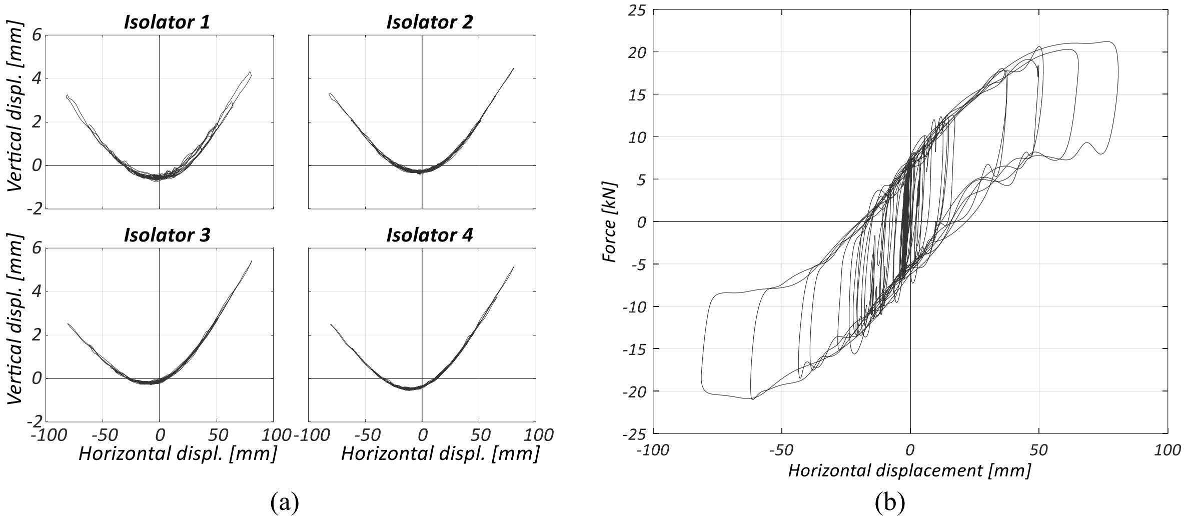

Figure 4: KSJ isolator performance in test run CIN250%-ISO: (a) trajectories of each device; (b) overall lateral hysteretic response under a superstructure weight of 205 kN.

Fig. 4b shows the hysteretic lateral force-displacement response for the entire system, with loops resembling those of friction-pendulum devices except for the variable slope associated with the KSJ variable-curvature trajectory. The lateral stiffness becomes zero at a lateral displacement of about 60 mm, where the trajectories show inflection points, confirming the analytical prediction. The loop width, measuring frictional resistance within pinned joints, was about 12 kN, denoting a frictional contribution of 6 kN. Subtracting friction effects, the restoring force for 80 mm of maximum lateral displacement was about 15 kN, consistent with the analytical prediction.

4.2 Isolation system effectiveness

The isolation effectiveness was evaluated in terms of elastic response spectra at 5% viscous damping ratio. Two acceleration signals were used: (i) the one recorded by the sensor on the shake-table, and (ii) the average of those recorded by the two accelerometers attached to the RC main mass. The ratio of the second to the first spectral ordinates was used to quantify the effectiveness of the isolation system in reducing or amplifying the demand imposed to the superstructure.

Fig. 5a shows that under the CIN250%-ISO input, the isolators reduce the spectral ordinates up to periods of about 1.0 s, while amplifying the demand on longer-period oscillators, with maximum amplification around 1.7 s: this corresponds to the average isolated period of $T_b \approx 1.8$ s predicted for a maximum displacement of 80 mm [23]. These observations support the prescription of the Italian building code [27], which allows the isolation system to be adopted for superstructures with fundamental period $T_s \leq 0.33 \cdot T_b = 0.6$ s.

The average period of the isolation system depends on the lateral displacement undergone by the KSJ devices, resulting in shorter average isolated periods for smaller displacements. Consequently, the spectral-reduction period range also depends on the displacement demand on the KSJ isolators, becoming narrower for lower-intensity input motions that impose smaller displacements on the isolators. For example, under CIN100%-ISO, the spectral-reduction range is limited to a maximum of 0.4 s (Fig. 5b).

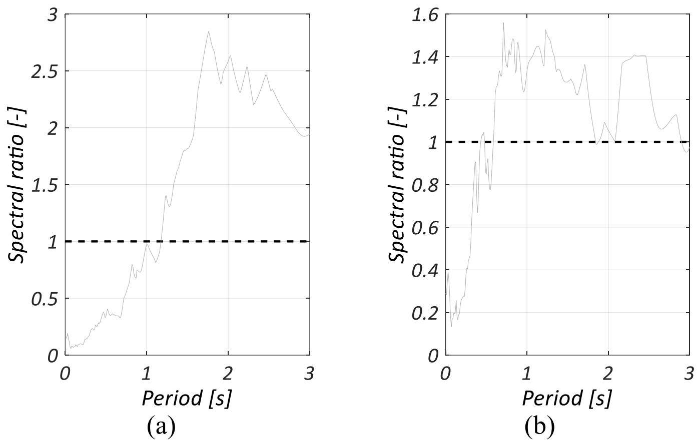

Figure 5: Isolation effectiveness: (a) test run CIN250%-ISO; (b) test run CIN100%-ISO.

4.3 Response of nonstructural elements

Incremental dynamic testing (IDT) curves were generated to evaluate the response of the rocking marble blocks and the museum showcase (Fig. 6 and Fig. 7). The horizontal peak ground acceleration (PGA) was used as the intensity measure for all non-structural components. The engineering demand parameter for the rocking blocks was taken as the maximum lateral displacement, normalized with respect to the critical value at the onset of static instability. The maximum top acceleration amplification, with respect to the shake-table acceleration, was used for the showcase.

The seismic isolation system was effective in preventing instability of the one-side-rocking block up to a PGA of 0.82 g (Fig. 6a and Fig. 7a). In fixed-base conditions during the EMN200%-FIX and EMN175%-FIX-Z tests, this same block exceeded its critical displacement for PGAs of 0.45 g and 0.43 g, respectively.

However, the isolation system was less effective for the free-rocking block (Fig. 6b and Fig. 7b), despite some displacement demand reduction under the same PGA. Safety steel cables limited this block's displacement to 80% of the critical value to prevent damage to nearby components, as shown by dashed vertical lines on Fig. 6 and Fig. 7; they were engaged in isolated configuration during test run EMN200%-ISO with a PGA of 0.49 g. It should be noted that this PGA was not reached when scaling the EMN record in fixed-base conditions. Additionally, imperfections at the base of the free-rocking block resulted in vibrations under PGAs lower than the theoretical rocking activation acceleration of 0.2 g.

The EMN signal was found to be more demanding than the CIN record for both rocking blocks of the test setup due to its frequency content. There were no observable effects on the rocking response related to the application of the vertical excitation component.

The isolation system significantly reduced the acceleration amplification of the museum showcase (Fig. 6c and Fig. 7c), independently of the input signal. The amplification decreased by a factor of 3 to 6, depending on the intensity of the ground motion. Application of the vertical acceleration history did not have any appreciable effect on the showcase response.

The behavior of the Michelangelo's David small-scale replica was less influenced by isolation: the statue fell during test runs EMN125%-ISO and EMN125%-FIX, for PGA slightly higher than 0.3 g in both cases. Adding the vertical excitation component anticipated its fall to PGA of 0.25 g during run EMN100%-FIX-Z.

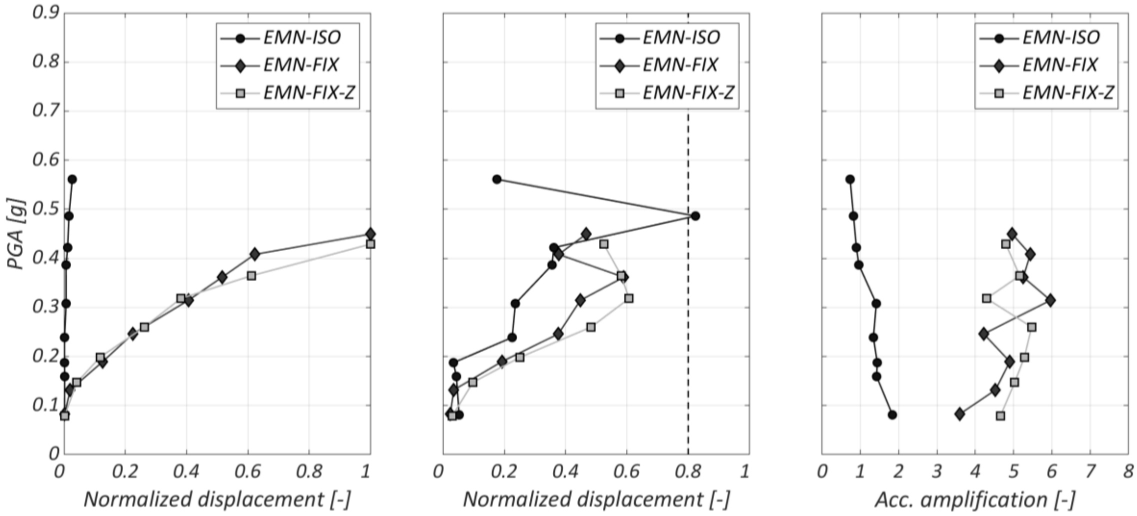

(a) (b) (c)

Figure 6: IDT curves for nonstructural elements under the EMN input sequences: (a) one-side-rocking block; (b) free-rocking block; (c) museum showcase.

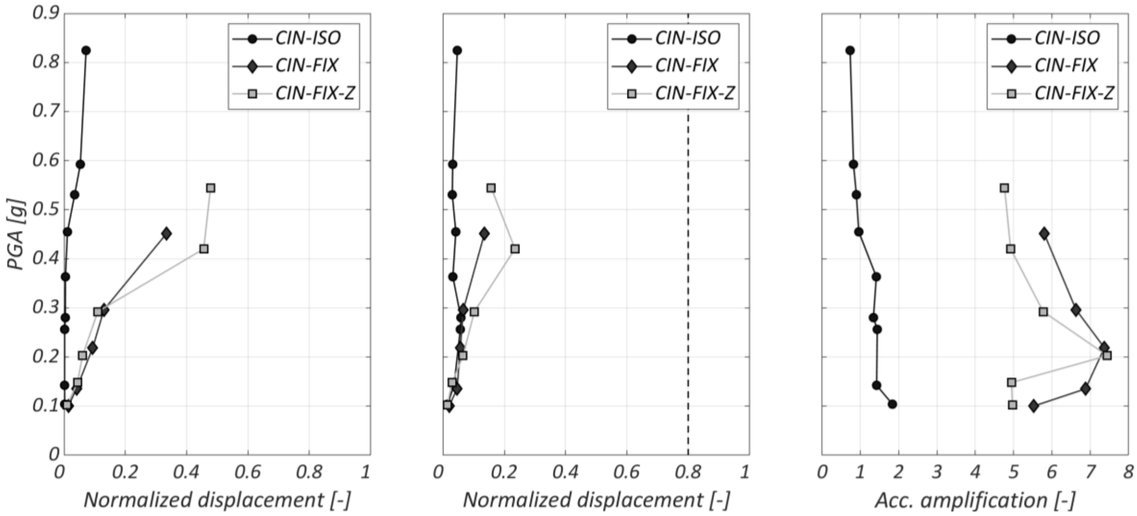

(a) (b) (c)

Figure 7: IDT curves for nonstructural elements under the CIN input sequences: (a) one-side-rocking block; (b) free-rocking block; (c) museum showcase.

5 CONCLUSIONS

The paper has discussed the effectiveness of an innovative seismic isolation device called "Kinematic Steel Joint" (KSJ) in protecting nonstructural cultural heritage components from earthquake-induced accelerations. Compared to other isolators on the market, the KSJ has competitive fabrication and maintenance costs because it consists of simply cut and folded steel sheets with pinned joints.

The results of an incremental, unidirectional dynamic shake-table test campaign confirmed the behavior of the proposed isolation technology predicted through an analytical formulation.

The KSJ isolator applied a restoring force proportional to the slope of the motion trajectory, consisting of upward and lateral displacements with recentering features, similarly to friction pendulum devices. The period of the isolated system was independent of the mass and related to the curvature of the trajectory, which was not constant. However, an average period could be estimated with the equation of a simple gravity pendulum, considering an average radius of curvature at the lateral displacement of interest.

The KSJ solution proved to be effective at reducing the seismic demand on the superstructure, over a period range that varies with the displacement demand imposed on the isolators. Additionally, the KSJ isolators provide some energy dissipation thanks to friction at the pinned joints.

The response of two rocking blocks and a museum showcase, mounted above the isolated mass, generally benefitted from the base-isolation system, compared to the fixed-base configuration. Tests conducted with fixed base under the same horizontal input sequence, combined with vertical excitation, resulted in a negligible influence of the latter.

The small-scale replica of Michelangelo's David statue, installed inside the showcase, was less sensitive to the presence of an isolation system; however, it was negatively affected by the application of the vertical component, which anticipated its fall from more than 0.3 g of PGA to about 0.25 g.

The experimental outcomes have confirmed the importance of protecting cultural heritage assets from earthquake-induced accelerations and the effectiveness of seismic isolation for this purpose. Overall, the KSJ solution is a promising development in the field of seismic protection for nonstructural components.

The results of this study encourage future developments of the KSJ isolator. Further investigations and geometric optimizations will allow reducing the size of the devices and obtaining lateral displacement ranges and trajectory curvatures compatible with a variety of building and nonstructural component configurations. For instances, studies have been conducted about KSJ applications to statues and industrial steel racks.

ACKNOWLEDGMENTS

The authors would like to thank Kyneprox S.r.l. for the financial and material collaboration in the development and testing of the proposed technology. The financial support to the experimental campaign provided by the EUCENTRE Foundation, within the project Mobartech (Regione Lombardia), and by Goppion S.p.A., is gratefully acknowledged. The valuable contributions of G. Ausenda, U. Tomassetti, G.C. De Sanctis, and the EUCENTRE Foundation laboratory staff are also duly appreciated.

REFERENCES

[1] Guerrini G, Restrepo JI, Massari M, Vervelidis A (2015). Seismic behavior of posttensioned self-centering precast concrete dual-shell steel columns. *Journal of Structural Engineering (ASCE)*, **141**(4), 04014115. DOI: 10.1061/(ASCE)ST.1943-541X.0001054.

[2] Ding D, Arnlod C, et al. (1990). Architecture, building contents, and building systems. *Earthquake Spectra*, **6**(1-suppl), 339-377. DOI: 10.1193/1.1585607.

[3] Filiatrault A, Sullivan T (2014). Performance-based seismic design of nonstructural building component. *Earthquake Engineering and Engineering Vibrations*, **13**(1-suppl), 17-46. DOI: 10.1007/s11803-014-0238-9.

[4] Di Sarno L, Petrone C, Magliulo G, Manfredi G (2015). Dynamic properties of typical consultation room medical components. *Engineering Structures*, **100**, 442-454. DOI: 10.1016/j.engstruct.2015.06.036.

[5] Spyrakos CC, Maniatakis CA, Taflampas IM (2017). Application of predictive models to assess failure of museum artifacts under seismic loads. *Journal of Cultural Heritage*, **23**, 11-21. DOI: 10.1016/j.culher.2016.10.001.

[6] Fragiadakis M, Kolokytha M, Diamantopoulos S (2017). Seismic risk assessment of rocking building contents of multistorey buildings. *Procedia Engineering*, **199**, 3534-3539. DOI: 10.1016/j.proeng.2017.09.507.

[7] Kelly TE (2001). *Base Isolation of Structures - Design Guidelines*. Holmes Consulting Group Ltd, Wellington, New Zealand.

[8] Sorace S, Terenzi G (2015). Seismic performance assessment and base-isolated floor protection of statues exhibited in museum halls. *Bulletin of Earthquake Engineering*, **13**(6), 1873-1892. DOI: 10.1007/s10518-014-9680-3.

[9] Gidaris I, Taflanidis AA, Lopez-Garcia D, Mavroeidis GP (2016). Multi-objective risk-informed design of floor isolation systems. *Earthquake Engineering & Structural Dynamics*, **45**(8), 1293-1313. DOI: 10.1002/eqe.2708.

[10] Caliò I, Marletta M (2003). Passive control of the seismic rocking response of art objects. *Engineering. Structures*, **25**(8): 1009-1018. DOI: 10.1016/S0141-0296(03)00045-2.

[11] Lowry M, Farrar BJ, Armendariz D, Podany J (2007). Protecting collections in the J. Paul Getty Museum from earthquake damage. *WAAC Newsletter*, **29**(3), 16-23.

[12] Vassiliou MF, Makris N (2012). Analysis of the rocking response of rigid blocks standing free on a seismically isolated base. *Earthquake Engineering and Structural Dynamics*, **41**(2), 177-196. DOI: 10.1002/eqe.1124.

[13] Baggio S, Berto L, Favaretto T, Saetta A, Vitaliani R (2015). Seismic isolation technique of marble sculptures at the Accademia Gallery in Florence: numerical calibration and simulation modelling. *Bulletin of Earthquake Engineering*, **13**(9), 2719-2744. DOI: 10.1007/s10518-015-9741-2.

[14] Chrysostomou CZ, Kyriakides N, Roussis PC, Asteris PG (2015). Emerging technologies and materials for the seismic protection of cultural heritage. In: *Handbook of Research on Seismic Assessment and Rehabilitation of Historic Structures*, Asteris PG and Plevris V, Eds., pp. 576-606, IGI Global. DOI: 10.4018/978-1-4666-8286-3.ch019.

[15] Podany J (2017). When Galleries Shake: Earthquake Damage Mitigation for Museum Collections. Getty Publications, Los Angeles, CA, USA. ISBN 978-1-60606-522-8.

[16] Froli M, Giresini L, Laccone F (2019). Dynamics of a new seismic isolation device based on tribological smooth rocking (TROCKSISD). *Engineering structures*, **193**, 154-169. DOI: 10.1016/j.engstruct.2019.05.014.

[17] Christopoulos C, Filiatrault A (2006). *Principles of Passive Supplemental Damping and Seismic Isolation*. IUSS Press, Pavia, Italy. ISBN: 88-85701-10-6.

[18] Lee DJ (1981). Recent experience in the specification, design, installation, and maintenance of bridge bearings. *Proc. World Congress on Joint Sealing and Bearing Systems for Concrete Structures*, Publication SP-70, Vol. 1, pp. 161-175, American Concrete Institute, Detroit, MI, USA.

[19] Kauschke W, Baigent M (1986). Improvements in the long term durability of bearings in bridges, especially of PTFE slide bearings. *Proc. 2nd World Congress on Joint Sealing and Bearing Systems for Concrete Structures*, Publication SP-94, Vol. 2, pp. 577-612, American Concrete Institute, Detroit, MI, USA.

[20] Clark PW, Kelly JM, Aiken ID (1996). Aging studies of high-damping rubber and lead-rubber seismic isolators. *Proc. 4th U.S.-Japan Workshop on Earthquake Protective Systems for Bridges*, Technical Memorandum No. 3480, 75-89, Public Works Research Institute, Ministry of Construction, Tokyo, Japan.

[21] Morgan T, Whittaker AS, Thompson A (2001). Cyclic behavior of high-damping rubber bearings. *Proc. 5th World Congress on Joints, Bearings and Seismic Systems for Concrete Structures*, Rome, Italy.

[22] Constantinou MC, Whittaker AS, Kalpakidis Y, Fenz DM, Warn GP (2007). *Performance of Seismic Isolation Hardware under Service and Seismic Loading*, Technical report MCEER-07-0012, MCEER, University at Buffalo, The State University of New York, Buffalo, NY, USA.

[23] Guerrini G, Ausenda G, Graziotti F, Penna A (2019). An innovative seismic isolation device based on multiple articulated quadrilateral mechanisms: analytical study and shake-table test. *Proc. 18th ANIDIS Conference*, Ascoli Piceno, Italy.

[24] Guerrini G, Graziotti F, Penna A (2023). Shake-table tests on an industrial steel rack isolated with innovative modular devices. In: *Seismic Isolation, Energy Dissipation and Active Vibration Control of Structures*, Cimellaro GP, Ed., Lecture Notes in Civil Engineering 309, pp. 853-863, Springer, Cham, Switzerland. DOI: 10.1007/978-3-031-21187-4_74.

[25] Alberti E, Ausenda G, Castino MC, Lo Iacono F, Navarra G (2023). Seismic protection of the Goddess of Morgantina statue through an innovative base-isolation device: validation by shake-table tests. In: *Seismic Isolation, Energy Dissipation and Active Vibration Control of Structures*, Cimellaro GP, Ed., Lecture Notes in Civil Engineering 309, pp. 717–725, Springer, Cham, Switzerland. DOI: 10.1007/978-3-031-21187-4_61.

[26] Luzi L, Pacor F, Puglia R (2019). *Italian Accelerometric Archive v3.0*. Istituto Nazionale di Geofisica e Vulcanologia, Dipartimento della Protezione Civile Nazionale. DOI: 10.13127/itaca.3.0.

[27] Ministero delle Infrastrutture e dei Trasporti (MIT) (2019). *Istruzioni per l'Applicazione dell'Aggiornamento delle "Norme Tecniche per le Costruzioni" di cui al Decreto Ministeriale 17 Gennaio 2018*, Circolare 21 gennaio 2019, n.7, C.S.LL.PP., Gazzetta Ufficiale della Repubblica Italiana, Rome, Italy (in Italian).